 DOI: 10.1002/masy.200750512

3D Networks from Self-Assembling Ionic-Complementary Octa-Peptides

Amran Mohammed,[1] *Aline F. Miller,*[2] *Alberto Saiani**[1,2]

Summary: The self-assembly and gelation properties of a set of four octo-peptides AEAEAKAK, AEAKAEAK, FEFEFKFK and FEFKFEFK based on alanine (A), phenylalanine (F), lysine (K) and glutamic acid (E) were investigated via small angle neutron scattering (SANS). The SANS experiments suggest that AEAKAEAK peptide does not self-assemble in solution while AEAEAKAK form rod-like structure i.e.: fibres with a radius of ~3.3 nm. The latter peptide does not form a gel suggesting that the fibres do not aggregate and form a three-dimensional network. On the other hand FEFEFKFK and FEFKFEFK peptides were found to form gels for concentrations higher than ~7 mg ml^{-1}. Below the critical gelation concentration these peptides were also found to form fibrillar structures with smaller average radii of ~1.7 nm. Above the critical gelation concentration a scattering maximum is observed in the scattered intensity curve. From the position of the maximum a rough estimation of the mesh size of the gel network could be derived and was found to vary between 15 and 30 nm depending on the gel concentration.

Keywords: fibres; gelation; hydrogels; network; peptide; SANS; self assembly; small angle neutron scattering

Introduction

Molecular self-assembly is a powerful tool for the preparation of molecular materials with a wide variety of properties. This is illustrated by the abundance of self-assembled proteins and polysaccharides encountered in Nature.[1–3] Peptides are particularly promising as building blocks for a number of reasons. The natural amino acid pool consists of 20 members with different physical properties including polar, non-polar, acid, basic and aromatic groups. In addition, an infinite number of unnatural amino acids can be designed in the laboratory. Amino acids can be combined in endless different ways leading to a vast number of building blocks with different physical properties.[4–6]

However, the understanding of the molecular interactions and self assembly rules in these materials is still limited, consequently the fundamental link between building block structure, mesoscopic structure and material properties has not yet been elucidated. We decided to focus our work on a set of so-called ionic-complementary peptides.[7] Since their discovery by Zhang ionic-complementary peptides have attracted considerable attention as they represent a potential new generation of natural biomaterials for applications such as 3-D scaffolds for tissue engineering or new drug delivery vehicles.[8,9] On a more fundamental note it is hoped that the investigation of these systems will help the understanding of amyloid fibrillogenesis in protein misfolding diseases (e.g. Alzheimer, Parkinson).

In our work we decided to undertake a systematic investigation of a series of

[1] School of Materials, The University of Manchester, Grosvenor Street, Manchester M1 7HS UK
E-mail: A.Saiani@manchester.ac.uk
[2] School of Chemical Engineering and Analytical Science, The University of Manchester, Sackville Street, P.O. Box 88, Manchester M60 1QD, UK

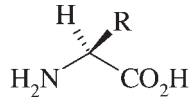

Alanine (A)	R = -CH_3	Phenylalanine (F)	R = -CH_2-Ph
Lysine (K)	R = -$(CH_2)_4$-NH_2	Glutamic Acid (E)	R = -$(CH_2)_2$ -COOH

Figure 1.
Chemical structure and nomenclature of amino acids used to formulate our peptides.

octa-peptides inspired from work by Caplan and co-workers.[10–12] The peptides were synthesized in our laboratory via solid phase synthesis methods[13] using the amino acids listed in Figure 1.

Alanine (A) and phenylalanine (F) are two non-charged amino acids, phenylalanine being more hydrophobic. These two amino acids were used to modify the overall hydrophobicity of the peptides. Lysine (K) and glutamic acid (E) are charged peptides and will carry a positive and a negative charge respectively at neutral pH. Four octo-peptides were synthesised: AEAEAKAK, AEAKAEAK, FEFEFKFK and FEFKFEFK; based on the alternation of one charged and one non-charged amino acid. The overall charge of the peptide was kept neutral in order to obtain a pH in between 6 and 7 when dissolved in water. The self-assembly and gelation properties of our peptides in water at different concentrations were subsequently investigated using small angle neutron scattering (SANS).[14,15]

Experimental Part

Synthesis

Amino acids, activator (HCTU) and Wang resin were purchased from Novabiochem (Merck) and used as received. All other reagents and solvents were purchased from Aldrich and used without further purification. The synthesis of the octo-peptides was done via standard solid-phase synthesis[13] using a ChemTech ACT 90 peptide synthesiser (Advance ChemTech Ltd., Cambridgeshire, UK). After cleavage from the resin and deprotection of the side groups and N-terminus using a TFA – anisole (95/5) mixture, the peptides were recovered in cold ether, centrifuged and freeze-dried. The synthesis yields ranged between 80 to 90%. A combination of HPLC chromatography and mass spectrometry were used to confirm the peptide structure and estimate their purity. The purity of all the octa-peptides synthesised was 90% or higher. The peptides were used with no further purification.

Solutions and Gel Preparation

Solutions and gels were prepared directly in Hellma quartz cells with an optical path length of 2 and 5 mm by dissolving the desired quantity of peptide in deuterated water at 90 °C. The solutions were agitated at high temperature for 10 to 20 minutes depending on the concentration and peptide used to ensure full dissolution. All the solutions had a pH between 6 and 7. The solutions were then cooled down at room temperature. Depending on the concentration and peptide used gelation occurred during cooling.

Small Angle Neutron Scattering

The experiments were carried out on KW2 and LOQ small-angle cameras located at JCNS, (Institut für Festkörperforschung, Julich, Germany) and at ISIS (Rutherford-Appleton Laboratory, Didcot, UK) respectively. The normalisation of the scattered intensities was performed using the standard procedures for each camera (further details are available on request at JCNS

and ISIS). The absolute intensities scattered by the peptides reads:[16]

$$I_A(q) = \frac{1}{K}[I_N(q) - (1 - C_P)I_D(q) - I_{inc}] \quad (1)$$

where I_N is the normalised intensity scattered by the sample, C_p the peptide concentration expressed in g cm^{-3}, I_D the normalized intensity scattered by the solvent, I_{inc} the incoherent scattering of the hydrogenous peptide and K the contrast factor expressed as:[16]

$$K = \frac{(a_p - Y_{ps}a_s)^2 N_A}{m_p^2} \quad (2)$$

where a_p and a_s are the scattering lengths of the peptide and the solvent respectively and Y_{ps} the molar volume ratio (v_p/v_s) between the peptide and the solvent. The molar volumes of the peptides were calculated by adding the molar volume values reported by Zaccai et al.[17] for each amino acid in the sequence. The peptide scattering lengths were calculated assuming that all labile hydrogens on the peptides were exchanged with deuterium.[17] By varying the sample-to-detector distance the available momentum transfer vector range, q, was $0.1 < q\ (\mathrm{nm}^{-1}) < 1.6$, q being defined as:

$$q = \frac{4\pi}{\lambda}\sin(\theta/2) \quad (3)$$

where θ is the scattering angle and λ the wavelength of the incident beam. In Figure 2 the scattering curves obtained for the alanine based peptides are presented in a logarithm representation. As can be seen from Figure 2 at high q values the scattering intensities become constant suggesting that the background scattering corresponding to the incoherent scattering of the hydrogenous peptide is observed, the incoherent scattering of the deuterated solvent being negligible. I_{inc} of the peptide was therefore estimated by averaging the last 10 points of the scattering curves.

Results and Discussion

Alanine Based Octo-peptides

In Figure 2 the normalised intensities scattered by the alanine based octa-peptides at different concentrations are presented in a logarithm representation. As can be seen for AEAEAKAK peptide a q^{-1}

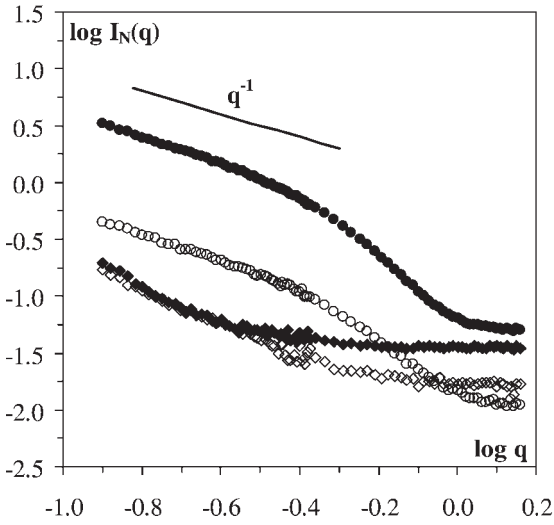

Figure 2.
log $I_N(q)$ vs. *log q* plot of the normalised intensities scattered by AEAKAEAK 10 mg ml^{-1} (◇), AEAKAEAK 40 mg ml^{-1} (◆), AEAEAKAK 10 mg ml^{-1} (○), AEAEAKAK 80 mg ml^{-1} (●) solutions.

slope is observed at low and intermediate q values at both concentrations (10 and 80 mg ml^{-1}) suggesting the presence of rod-like structures in this system. At high q values $I_N(q)$ becomes constant suggesting, as said previously, that at high q values the incoherent scattering of the hydrogenous peptide is observed. For the AEAKAEAK peptide a weak increase in $I_N(q)$ is observed at low q values where the scattering intensities seem to become independent of the sample concentrations (10 and 40 mg ml^{-1}). This suggests that the scattering observed at low q values does not correspond to the peptide and is probably due to a low level contamination of the sample by large size objects. At intermediate and high q values $I_N(q)$ becomes dependent on the concentration of the samples. The scattering observed being weak and constant suggests that the scattering observed simply corresponds to the incoherent scattering of the hydrogenous peptide. These results suggest that for the AEAEAKAK peptide self-assembly occurs and higher ordered rod-like structures i.e.: fibres form, while for the AEAKAEAK peptide no self-assembly occurs.

For rod-like structures when $qR_\sigma < 1$, R_σ being the cross-section radius of gyration of the rod, the scattered intensity can be written as:[16]

$$qI_A(q) = \pi C_p \mu_L \exp(-q^2 R_\sigma/2) \quad (4)$$

where μ_L is the linear mass of the rod. The presence of rod-like structures can be confirmed by plotting the absolute scattered intensity, $I_A(q)$, by means of a $qlnI_A(q)$ *vs* q^2 representation as shown in Figure 3. The presence of a linear behaviour at low q is characteristic of the presence of rod-like structures. From the slope of the line and the intercept with the y axes R_σ and μ_L can be estimated. The following values where obtained:

AEAEAKAK
80 mg ml^{-1} $R_\sigma = 2.4 \pm 0.3$ nm
$\mu_L = 2350 \pm 300$ g mol^{-1} nm^{-1}
10 mg ml^{-1} $R_\sigma = 2.2 \pm 0.3$ nm
$\mu_L = 2460 \pm 300$ g mol^{-1} nm^{-1}

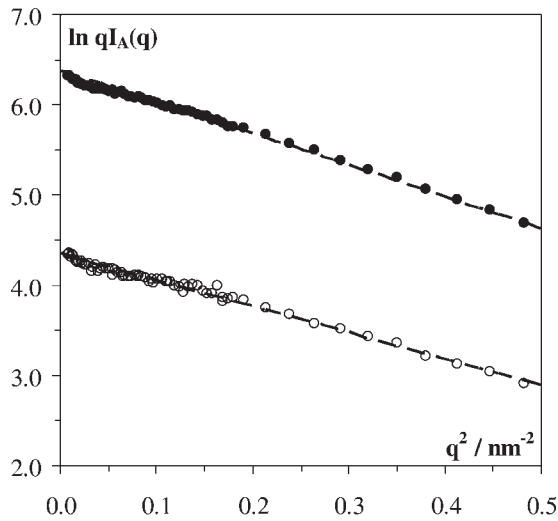

Figure 3.
ln qI_A (q) vs. q^2 plot of the intensities scattered by AEAEAKAK 10 mg ml^{-1} (○), AEAEAKAK 80 mg ml^{-1} (●) solutions.

The same values for R_σ and μ_L were obtained at both concentrations suggesting that similar rod-like structures are formed.

At low resolution the scattering of rod-like structures or fibres can be approximated by the scattering of infinitely long plain cylinders with scattered intensity:[16]

$$q^2 I_A(q) = 4\pi q \mu_L C_p \left(\frac{J_1(qr)}{qr}\right)^2 + Cst \qquad (5)$$

where r is the radius of the cylinder, Cst a constant term taking into account interscattering effects and J_1 the first order Bessel function. In Figure 4 the absolute scattered intensity of AEAEAKAK peptide solutions are presented by mean of a Kratky representation ($q^2 I_A(q)$ vs. q) with the best fit obtained using Equation (5) (dotted lines). As can be seen very good fits are obtained at both concentrations using this plain-cylinder model. From the fitting the radius and the linear mass of the rods can be obtained:

The values obtained for the linear mass of the rods are in very good agreement with the values obtained previously. For a plain-cylinder model the radius of the cylinder and its cross-section radius of gyration are related through:

$$R_\theta = \sqrt{\frac{r^2}{2}} \qquad (6)$$

In this case a very good agreement is again obtained between the value obtained for r using the plain-cylinder model and the value estimated previously for R_σ.

These results also suggest that even at high concentrations (80 mg ml^{-1}) the system can be described by a dilute solution of rod-like structures (i.e.: fibres) as no interscattering effects are observed. This would imply that no association through specific interactions between the rods/fibres occurs. This is confirmed by the fact that no gel, as defined by Guenet and coworkers,[3,18] is obtained for AEAEAKAK

AEAEAKAK	80 mg ml^{-1}	$r = 3.4 \pm 0.4$ nm
		$\mu_L = 2180 \pm 400$ g mol^{-1} nm^{-1}
	10 mg ml^{-1}	$r = 3.2 \pm 0.4$ nm
		$\mu_L = 2370 \pm 400$ g mol^{-1} nm^{-1}

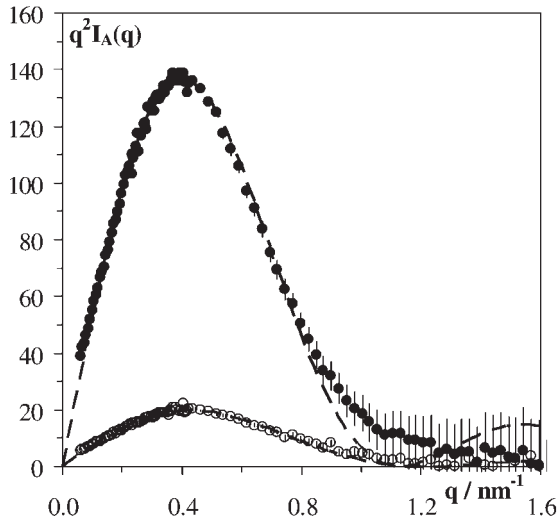

Figure 4.
Kratky ($q^2 I_A(q)$ *vs* q) plot of the intensities scattered by AEAEAKAK 10 mg ml^{-1} (○), AEAEAKAK 80 mg ml^{-1} (●) solutions. The dotted line represent the best fit obtained using the plain cylinder model (Equation 5).

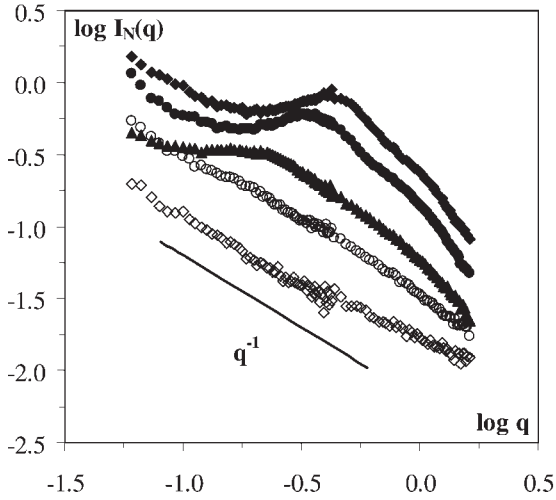

Figure 5.
log $I_N(q)$ vs. *log q* plot of the normalised intensities scattered by FEFEFKFK peptide samples at 2 mg ml^{-1} (◇), 5 mg ml^{-1} (○), 10 mg ml^{-1} (▲), 30 mg ml^{-1} (●) and 40 mg ml^{-1} (◆).

peptide at any concentrations. Instead viscous solutions are obtained as expected for entangled fibres. For the AEAKAEAK peptide very low viscosity solutions are obtained as expected for a non self-associating system where the peptide is simply dissolved.

Phenylalanine Based Octa-Peptides

The normalised intensities scattered by the phenylalanine based octo-peptide FEFEFKFK are presented in Figure 5 at different concentrations (2, 5, 10, 30 and 40 mg ml^{-1}) are presented in a logarithm representation. The same results were obtained for the FEFKFEFK peptide (data not shown).

For phenylalanine based peptides gelation occurs for concentrations higher than ~7 mg ml^{-1}. Gelation results in the presence of a maximum in the scattering intensity curve as can be seen from Figure 6

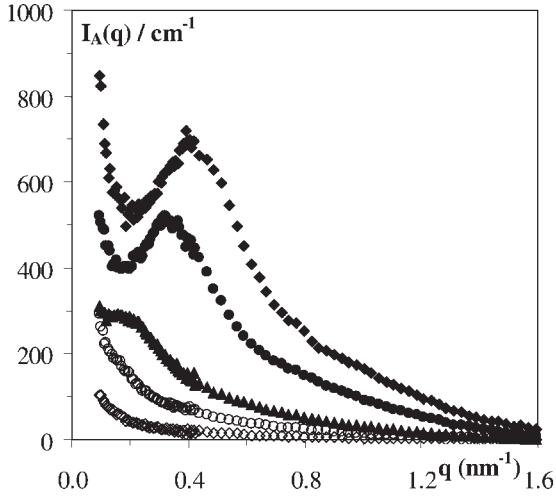

Figure 6.
$I_A(q)$ vs. *q* plot of the absoluted intensities scattered by FEFEFKFK peptide samples at 2 mg ml^{-1} (◇), 5 mg ml^{-1} (○),10 mg ml^{-1} (▲), 30 mg ml^{-1} (●) and 40 mg ml^{-1} (◆).

where $I_A(q)$ is plotted as a function of q for all the samples. A rough estimation of the gel mesh size, d, can be obtained from the position of the maximum through the Bragg relation:

$$d = \frac{2\pi}{q*} \tag{7}$$

where q^* is the position of the intensity maximum. The mesh size was found to decrease with increasing concentration from 30 to 15 nm.

Below the critical gelation concentration viscous solutions are obtained and the respective scattering curves show a q^{-1} behaviour suggesting the presence of rod-like structures.

This can clearly be seen for 2 and 5 mg ml^{-1} samples in Figure 5. The same analysis as used for the alanine based peptide can be performed for these two samples. In Figure 6 the absolute scattered intensities are presented in a Kratky representation with the best fit obtained using the plain cylinder model described by Equation (5). The scattering curves, as shown in Figure 7, are well reproduced using this model. From the fits the rod radius as well as the rod linear mass can be derived:

AEAEAKAK	2 mg ml^{-1}	$r = 1.7 \pm 0.5$ nm
		$\mu_L = 1420 \pm 400$ g mol^{-1} nm^{-1}
	5 mg ml^{-1}	$r = 1.7 \pm 0.5$ nm
		$\mu_L = 1950 \pm 400$ g mol^{-1} nm^{-1}

The same values are roughly obtained for both concentrations. These results suggest that at low concentration the phenylalanine based peptides self-assemble to form rod-like structures i.e.: fibres. At higher concentration these fibres self-assemble to form a three-dimensional network resulting in the physical gelation of the sample.

The characteristic fibre size obtained from our SANS data for the FEFEFKFK peptide (r ~ 1.7 nm) is half of the equivalent value obtained for the AEAEAKAK peptide (r ~ 3.4 nm).

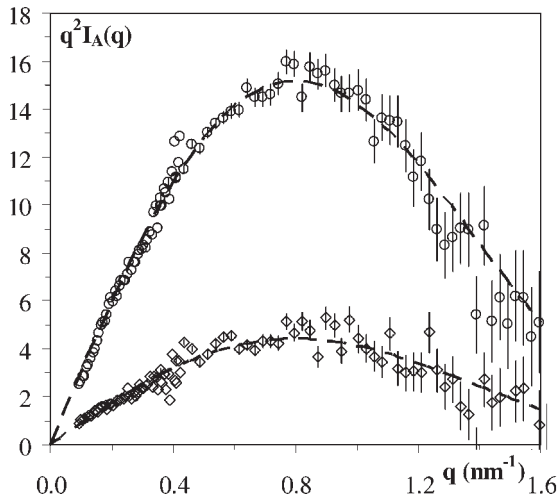

Figure 7.
Kratky ($q^2I_A(q)$ *vs* q) plot of the intensities scattered by FEFEFKFK 2 mg ml^{-1} (◇), FEFEFKFK 5 mg ml^{-1} (○) solutions. The dotted line represent the best fit obtained using the plain cylinder model (Equation 5).

If the fully extended conformation is assumed the length of our peptide is ~3.2 nm. This suggest that for the FEFEFKFK peptide the fibre diameter corresponds to one peptide unit while for the AEAEAKAK peptide it corresponds to two peptide units. This indicates that very different fibre structures are obtained for these two peptides suggesting a different self-assembling process. This is confirmed by the fact that FEFEFKFK forms physical gels at higher concentrations while AEAEAKAK did not form gels in the concentration range investigated.

Conclusion

We have investigated the self-assembly and gelation properties of a set of four octopeptides: AEAEAKAK, AEAKAEAK, FEFEFKFK and FEFKFEFK. No self-assembly was observed for AEAKAEAK while SANS results suggest fibres form from AEAEAKAK. The scattering curves could be fitted using a plain-cylinder model giving a fibre radius of ~3.3 nm. In the concentration range investigated no gelation was observed for the AEAEAKAK peptide suggesting that these fibres do not aggregate to form a three-dimensional network. The phenylalanine based peptides on the other hand were found to gel at concentrations greater than ~7 mg ml^{-1}. Below the critical gelation concentration these peptides were also found to form fibrillar structures with a smaller average radius of ~1.7 nm. Above the critical gelation concentration a scattering maximum is observed in the scattered intensity curve. From the position of the maximum a rough estimation of the mesh size of the gel network could be derived and was found to vary between 15 and 30 nm depending on the gel concentration.

Acknowledgements: The authors are grateful to Dr. H. Frielinghaus from JCNS (Institut für Festkörperforschung, Julich, Germany) and Dr. S. King from ISIS (Rutherford-Appleton Laboratory, Didcot, UK) for their support in the use of KW2 and LOQ small angle cameras respectively.

[1] H. Yan, A. Saiani, J. E. Gough, A. F. Miller, *Biomacromolecules* **2006**, *7*, 2776–2782.
[2] R. Langer, D. A. Tirrell, *Nature* **2004**, *428*, 487–492.
[3] J.-M. Guenet, *Thermoreversible Gelation of Polymers and Biopolymers*, Academic Press, London **1992**.
[4] R. J. Mart, R. D. Osborne, M. M. Stevens, R. V. Ulijn, *Soft Matter* **2006**, *2*, 822–835.
[5] V. Jayawarna, M. Ali, T. A. Jowitt, A. E. Miller, A. Saiani, J. E. Gough, R. V. Ulijn, *Advanced Materials* **2006**, *18*, 611– +.
[6] D. Lloyd-Williams, F. Albericio, E. Giralt, *Chemical Approaches to the Synthesis of Peptides and Proteins*, CRC Press, **1997**.
[7] P. Chen, Colloids and Surfaces a-Physicochemical and Engineering Aspects. **2005**, *261*, 3–24.
[8] S. G. Zhang, *Biotechnology Advances* **2002**, *20*, 321–339.
[9] S. G. Zhang, *Nature Biotechnology* **2003**, *21*, 1171–1178.
[10] M. R. Caplan, D. A. Lauffenburger, *Ind. Eng. Chem. Res.* **2002**, *41*, 403–412.
[11] M. R. Caplan, E. M. Schwartzfarb, S. G. Zhang, R. D. Kamm, D. A. Lauffenburger, *J. Biomater. Sci.-Polym. Ed.* **2002**, *13*, 225–236.
[12] M. R. Caplan, E. M. Schwartzfarb, S. G. Zhang, R. D. Kamm, D. A. Lauffenburger, *Biomaterials* **2002**, *23*, 219–227.
[13] W. C. W. P. D. Chan, *Fmoc Solid Phase Peptide Synthesis: A Practical Approach*, Oxford University Press, **1999**.
[14] A. Saiani, J. M. Guenet, *Macromolecules* **1997**, *30*, 966–972.
[15] A. Saiani, J. M. Guenet, *Macromolecules* **1999**, *32*, 657–663.
[16] J. S. Higgins, H. C. Benoit, *Polymer and Neutron Scattering*, Clarendon Press, Oxford **1994**.
[17] B. Jacrot, G. Zaccai, *Biopolymers* **1981**, *20*, 2413–2426.
[18] C. Daniel, C. Dammer, J.-M. Guenet, *Polymer* **1994**, *35*, 4243–4246.

